

**Self-assembled nucleo-tripeptide hydrogels provide local  
and sustained doxorubicin release**

Journal:	<i>Biomaterials Science</i>
Manuscript ID	BM-ART-01-2020-000134.R1
Article Type:	Paper
Date Submitted by the Author:	02-Mar-2020
Complete List of Authors:	Baek, Kiheon; The University of Texas at Austin OnRamps, Biomedical Engineering Noblett, Alexander; The University of Texas at Austin OnRamps, Biomedical Engineering Ren, Pengyu; The University of Texas at Austin OnRamps, Biomedical Engineering Suggs, Laura; University of Texas at Austin Cockrell School of Engineering, Biomedical Engineering

## **Self-assembled nucleo-tripeptide hydrogels provide local and sustained doxorubicin release**

*Kiheon Baek, Alexander David Noblett, Pengyu Ren, and Laura J. Suggs\**

Department of Biomedical Engineering, The University of Texas at Austin, 107 W Dean Keeton St, Austin, TX, 78712

Keywords: biocompatible materials, cancer therapy, drug delivery, injectable hydrogel, nucleopeptide

Self-assembled nucleo-peptide hydrogels have a nanofibril structure composed of noncovalent molecular interactions between peptide groups as well as  $\pi$ - $\pi$  stacking and Watson-Crick interactions via complementary nucleobases. These hydrogels have specific benefits for biomedical applications due to their DNA-like interactions in addition to the well-known advantages of peptide biomaterials: biocompatibility, extracellular matrix (ECM)-like structure, and bottom-up design. Inspired by the nucleobase stacking structure, we hypothesized that nucleo-peptides would be able to deliver the DNA-intercalating chemotherapeutic, doxorubicin (Dox) in a sustained manner when delivered locally to a solid tumor. Ade-FFF nucleo-peptide hydrogels were able to load a high concentration of Dox (1 mM) and demonstrated continuous release under in vitro degradation conditions. We adopted an in vivo tumor-bearing mouse model to evaluate the delivery of Dox by Ade-FFF hydrogels. We found that Dox-containing hydrogels reduced tumor growth and resulted in greater apoptosis-mediated cell death in the tumor as evidenced by caspase-3 expression. Pharmacokinetics and biodistribution studies also supported the observation that Dox delivery by an Ade-FFF hydrogel improves sustained delivery in the local tumor site. This study demonstrates the potential of self-assembled nucleo-peptides in biomedical applications by using their distinctive DNA-like structure.

## 1. Introduction

Controlled drug delivery allows for the transport and release of agents at the target site and with desirable kinetics in order to overcome limitations associated with bioavailability and challenges in pharmaceutical formulation. Diverse materials—synthetic and natural polymers, proteins, inorganic nanoparticles—and structures including vesicles, micelles, and fibers have been studied to construct novel drug delivery systems.<sup>[1-4]</sup> Hydrogels are a potential carrier for controlled drug delivery at local tissue sites. They create reservoirs at the target region, store drugs, and release them over continuous periods.<sup>[5-7]</sup> These highly hydrated (70-99%) materials form molecular or supramolecular networks and are made with synthetic, natural molecules, or both. Several characteristics of hydrogels—physical and chemical properties, size of mesh and architecture, and molecular interactions between network and drugs—are tunable and enable the formulation of appropriate drug release behavior based on accumulated studies.<sup>[3,8,9]</sup>

Supramolecular peptide hydrogels have recently emerged as candidates in biomimetics biomaterials design. Peptide hydrogels, which can form molecular networks via covalent interactions such as amide and disulfide bonds or secondary associations, are generally soft materials but due to a variety of chemical and biological characteristics can span a broad range of biomedical applications.<sup>[10,11]</sup> Peptide synthesis is well-established, and broad tunability and availability of biomimetic approaches make peptide hydrogels versatile. These strengths have enabled significant drug delivery research using peptide hydrogels for the past two decades. Peptide hydrogels form an extracellular matrix (ECM)-like network and therefore act as a biocompatible drug depot. Many drugs, from small molecules to large proteins, are effectively stored and released with highly controlled kinetics through diverse methods including diffusion, molecular interactions, and degradation-mediated release.<sup>[12-14]</sup>

In this study, a short nucleo-peptide hydrogel was used for sustained and efficient local cancer drug delivery. Formation of higher order structures was discussed in two recent reports.<sup>[17,19]</sup> We demonstrated that nucleo-peptide monomers associate primarily through hydrogen bonding and nucleobase stacking interactions. These individual groupings continue to aggregate into short, second order fibril-like assemblies. We have used amphiphilicity and solvent-accessible surface area as metrics to explain higher-order associations between fibrils into nanoscale fibers with hydrophobicity driving structure formation. Phenylalanine residues on peptides provide those properties at both second and third dimensions, while hydrophilic nucleobases attract and entrap water to form macroscale constructs, a condition that allows each region of the aggregates to exist in its most thermodynamically favored state. The structural and design similarities of AdeFFF used in this study led us to implicate a similar mechanism of self-assembly.

Long-term local delivery is required for inoperable cancers and tumor recurrence prevention.<sup>[15,16]</sup> High drug concentration and efficient release are necessary for continuous drug delivery to cancerous regions. Our group previously developed and characterized a family of self-assembling nucleo-tripeptide hydrogels, demonstrating that they formed nano-fibers having DNA-like structure through Watson-Crick interactions and nucleobase stacking.<sup>[17]</sup> Gelation of nucleo-tripeptides is controlled by pH change and their hydrogels undergo proteinase-mediated degradation. The activity of several cancer drugs, including doxorubicin (Dox), methanesulfonm-anisidide (mAMSA), and ellipticine, rely on a DNA intercalation mechanism, which result from the high affinity of planar ring structures.<sup>[18]</sup> Herein, we evaluated the chemotherapeutic (Dox) storage capacity of nucleo-tripeptide hydrogels via DNA intercalation and analyzed in vitro and in vivo drug release and kinetics.

## 2. Results and Discussion

### 2.1. Gelation of Ade-FFF nucleo-peptide

Ade-FFF formed a hydrogel by a pH switch method when the concentration was above the critical gelation concentration (0.45wt% = 7.087mM) as observed previously<sup>[17]</sup>. Self-assembled hydrogels were made at pH 7.5, and gelation was confirmed by vial inversion.

### 2.2. Loading capability and capacity analysis of Ade-FFF hydrogel

We hypothesized that nucleobase stacking structures in self-assembled nano-fibers store molecules that intercalate DNA, and we chose 4',6-diamidino-2-phenylindole (DAPI), a fluorescent dye used for nuclear visualization, to evaluate this phenomenon. Ade-FFF and DAPI-containing Ade-FFF hydrogels were both prepared and each was transferred to one side of a partitioned well in a 24-well plate. Both hydrogels reformed by self-healing and the partition was removed after five minutes. Phosphate-buffered saline was placed on top of the hydrogels and fluorescence imaging was performed to observe diffusion of DAPI (**Figure S1**). We detected a clear boundary during the first week and this was followed by a slow diffusion of DAPI across to the unloaded side. This preliminary study demonstrates the efficient loading capability of Ade-FFF hydrogels for molecules able to intercalate between nucleobases.

A Dox loading test for Ade-FFF hydrogels was then performed by mixing in a concentrated drug solution with the mechanically degraded construct. The Ade-FFF (final concentration: 25 mM) hydrogel was able to store 1 mM of Dox by recovering and maintaining its hydrogel form (**Figure 1**).

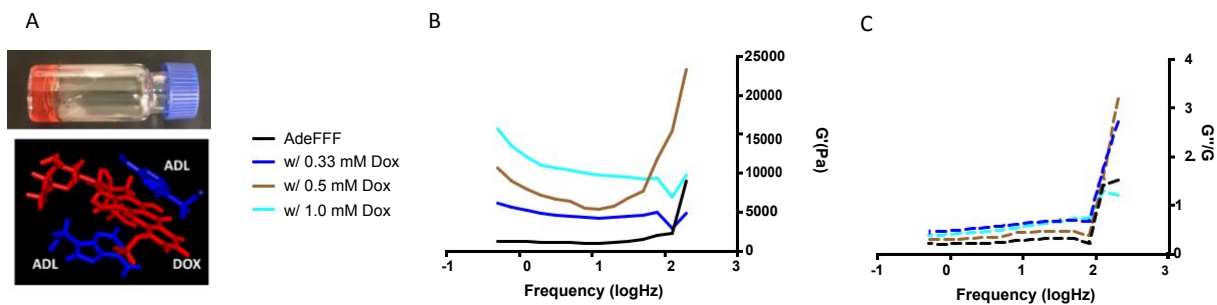


**Figure 1.** Ade-FFF hydrogel containing Dox (1 mM) maintained its hydrogel form (top), and MD simulation of Ade-FFF self-assembly with Dox showed drug intercalation between adenine stacking structures (bottom) (A). Storage moduli ( $G'$ ) of Ade-FFF hydrogels was greater with higher concentrations of Dox (B) and  $\tan(\delta)$  ( $G''/G'$ ) of Dox-containing hydrogels demonstrates viscoelastic properties (C).

### 2.3. Characterization of Dox containing Ade-FFF hydrogel

Previously, we characterized Ade-FFF self-assembly into nanofibrous hydrogels. Nucleobase stacking interactions were detected from the assembled structures (17). Additionally, our previous study compared self-assembling peptides and depsipeptides and indicated that hydrophobic interactions involving aromatic  $\pi$ - $\pi$  stacking mainly contributed to the self-assembly of short peptide derivatives.<sup>[19]</sup> From these results, we hypothesized that Dox would be efficiently loaded into the Ade-FFF hydrogels and that this interaction would be mediated by nucleobase stacking structures. Furthermore, we postulated that intercalation would enhance the strength of  $\pi$ - $\pi$  interactions, thus increasing the stiffness of the entire nanofibrous network.

We investigated whether or not Dox contributed to the self-assembly process by evaluating the mechanical properties of Ade-FFF hydrogels containing different Dox concentrations (0.33 mM to 1 mM) using rheometry (Figure 1). The results showed that adding Dox did indeed increase the storage modulus of Ade-FFF hydrogels up to 10 kPa, which is approximately 10 times stiffer than Ade-FFF alone. Molecular dynamics (MD) simulation was performed to determine if Dox is present within stacked nucleobases at an atomistic scale (**Figure 1**). A 50 ns simulated annealing of the system having randomly distributed 60 molecules of Ade-FFF and 15 molecules of Dox was performed, and  $\pi$ - $\pi$  stacking structures were analyzed. We found that the majority of Dox (8 molecules) forms  $\pi$ - $\pi$  interactions with adenine residues and several of the Dox molecules are located between adenine rings, thus forming intercalated structures (Figure S2). Additionally, the remaining Dox molecules formed  $\pi$ - $\pi$  interactions with phenylalanine residues or themselves.

Overall, the Ade-FFF hydrogel showed efficient Dox loading while maintaining its form and Dox enhanced the molecular interactions within the self-assembled structure by conferring greater  $\pi$ - $\pi$  interactions.

#### 2.4. In vitro Dox release from Ade-FFF hydrogels and release profile analysis

Many Dox delivery carriers have used covalent bonds or hydrophobic interactions to hold and release Dox.<sup>[20-23]</sup> These strategies have certain advantages, but they require additional chemical synthesis and purification steps or exhibit a burst effect with high Dox concentration when the interaction between the carrier and drug is weak.

Based on our DAPI diffusion test, drug loading and rheometry experiments, and molecular dynamics simulation study of Ade-FFF/Dox self-assembly, we suspected that release kinetics would be dominated by hydrogel degradation due to the strong molecular interactions between the reagent and assembled nanofibers. An in vitro release study under three different solution conditions—PBS, trypsin, and proteinase K—was performed to evaluate Dox delivery by Ade-FFF hydrogels (**Figure 2**). We detected minimal drug release from hydrogels in the PBS and trypsin groups. This supported our supposition that diffusion has a minor contribution to the release profile. Trypsin does not degrade the self-assembled structure of Ade-FFF because it generally cleaves the amide bond of lysine or arginine, which both have a charged side group. On the other hand, continuous Dox release was observed in the proteinase K group, which predominantly degrades peptide bonds in aromatic amino acids as in Ade-FFF molecules. About 55% of Dox was released over 12 days and the release profile followed a near linear curve ( $R^2=0.9366$ ). Our results show that Dox release is only allowed during bulk degradation of the self-assembled nucleo-peptide hydrogel. Mechanical properties of hydrogels in each treatment condition were measured. We observed that those treated with PBS and trypsin demonstrate long-term stability, while the proteinase K group shows a decrease in storage modulus over time that explains gradual drug release kinetics over the study period.

Dox release by the Ade-FFF hydrogel was also measured in the presence of 4T1 mice breast cancer cells. To analyze the effect of the drug, Dox-containing hydrogels were physically separated from cells by isolating constructs within a cell culture insert (Figure 2). On day 1, the viability of 4T1 cells in the Dox-solution group was reduced to around 20%, but the Dox/hydrogel group did not decrease viability because the hydrogel was not degraded. However, a reduced viability—50% on day 3 and 20% on day 5—was observed at longer timepoints in the Dox/hydrogel group, and the Dox/hydrogel group still contained 63% (0.317 mM) of Dox on day 5. This study indicated that a high concentration of Dox can inhibit cancer growth directly, but Dox delivery via Ade-FFF is able to decrease cancer cell survival and prevent the growth over time.

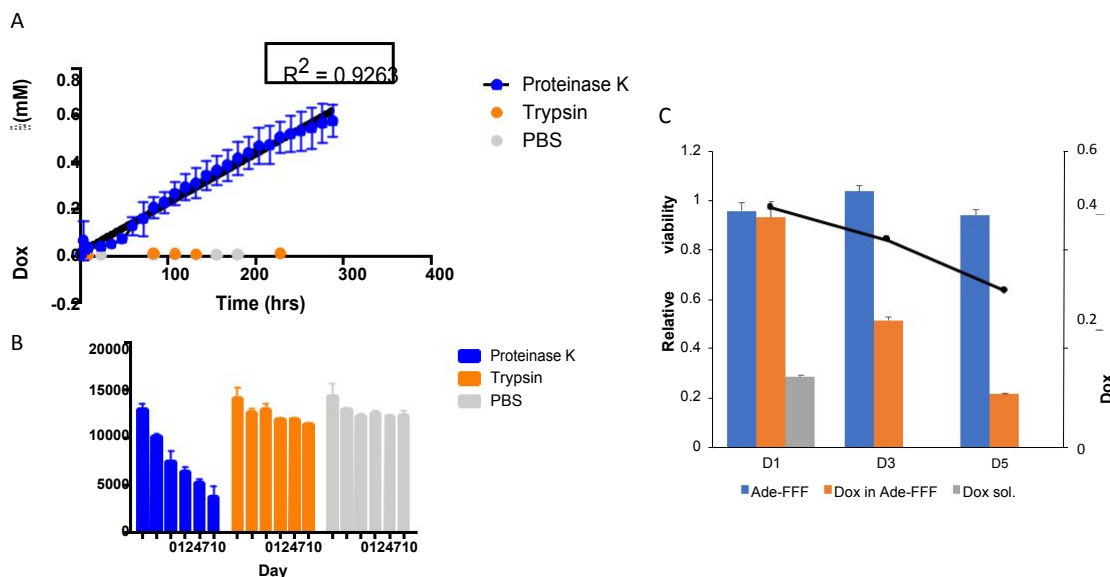


**Figure 2.** *In vitro* Dox release under several proteinase conditions showed that Dox was only released in proteinase K environment through enzyme-mediated degradation of the Ade-FFF hydrogel, which correlated with changes in mechanical properties after enzyme treatment (A and B). *In vitro* Dox release from Ade-FFF hydrogels in culture with 4T1 cells. Dox solution effectively killed all cancer cells, but Dox release from Ade-FFF hydrogels reduced 4T1 viability to below 20% using 37% of the initial amount of drug, indicating sustained release (C).

## 2.5. *In vivo* Dox release model with Ade-FFF hydrogel in mice

We used a BALB/c mouse model to study *in vivo* Dox release from an Ade-FFF hydrogel. A systemic toxicity test of the Ade-FFF hydrogel was initially performed by injecting it into the mouse mammary fat pad. Based on our examination of health status for 7 days and a histological study of the tissue surrounding the injected hydrogel, we did not identify any measurable systemic toxicity from the Ade-FFF construct relative to controls.

Next, the survival curve and tumor volume of mice in four groups (n=7) treated by PBS, hydrogel, Dox/sol, and Dox/gel were investigated for 12 days after intratumoral injection (**Figure 3**). We found that Dox-treated mice had longer survival times than animals from the control groups (treated by PBS or unloaded hydrogel). Additionally, a small, but significant difference was observed between the survival fraction of Dox/hydrogel and Dox/sol groups. Tumor volume increase in Dox/gel treated mice was significantly smaller than that of Dox/sol on day 12. This supports the conclusion that Dox was released in a continuous and efficient manner by the Ade-FFF hydrogel over the period of the study compared to local Dox delivery in solution. We also confirmed that there was a significant difference in tumor weight between Dox/gel and Dox/sol groups upon termination of the study. This *in vivo* Dox release study demonstrated increased Dox storage and sustained release from Ade-FFF hydrogels.

Immunohistochemical (IHC) staining against caspase-3 was performed on collected tumor tissue sections to further analyze the effectiveness of Dox delivery via Ade-FFF hydrogels. Dox induces caspase-3 activation in tumor cells, inhibiting the cell cycle and leading the apoptosis via p53 pathway.<sup>[24]</sup> Thus, the IHC of tumor tissues with caspase-3 binding antibody will indicate the effect of Dox treatment. Contrary to PBS or unloaded hydrogel-treated mice, cleaved caspase-3 positive cells were detected in stained tumor tissues of mice treated with Dox (Dox/sol and Dox/gel)

(**Figure 3**). Between the Dox/sol and Dox/gel groups, we observed a greater number of stained cells in the latter, indicating the efficacy of local Dox delivery via the Ade-FFF hydrogel.

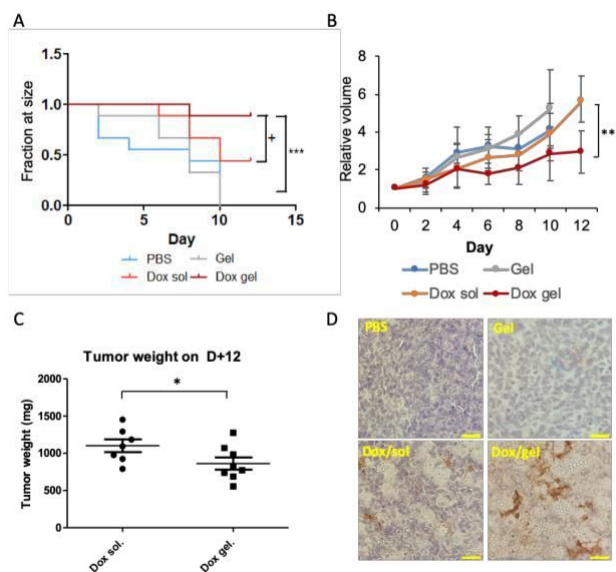


**Figure 3.** Survival curve of mice (A) and tumor growth curve (B) by *in vivo* Dox release showed that Dox/gel reagent could interrupt tumor activity and growth effectively. This was also supported by significantly different tumor weights between Dox/sol and Dox/gel group on day 12 (C). Images of IHC staining indicate more cells undergoing apoptosis after Dox/gel treatment (scale bar = 25 μm) (D).

## 2.6. Pharmacokinetics and biodistribution study of Dox treatment with Ade-FFF hydrogel

Pharmacokinetics and biodistribution of Dox during *in vivo* release were investigated to study the drug delivery profile. We examined 6 time points—hour 1, day 1, 2, 4, 6, and 8—and compared the injected hydrogel or solution (Dox/gel or Dox/sol). At 1 hour following treatment, we found that there was a different distribution of Dox around the tumor that was dependent on whether it was delivered in the hydrogel or in solution (**Figure 4**). The Dox-containing Ade-FFF hydrogel was detected next to tumor tissue, but the Dox/sol group showed dispersed reagent along the leg and abdominal regions in mice. We did not find the Ade-FFF hydrogel intact with loaded Dox after day 1, but the Dox/gel group also did not show diffused drug, as shown in Dox/sol group, at later time points.

The concentrations of Dox in plasma and tumor tissue were analyzed by collecting blood and organs at specific timepoints (**Figure 4**). Initially, a higher Dox concentration in plasma was observed in the Dox/sol group up to day 2, after which a similar quantity of Dox was detected in both the Dox/sol and the Dox/gel groups. We did find significantly different Dox concentrations in tumor tissue when comparing those two groups, however, and for the first 6 days, tumor tissue in the Dox/gel group contained a greater amount of drug. From these results, we determined that drug released from the Dox-loaded Ade-FFF hydrogel was able to persist in the tumor tissue longer, thus limiting tumor growth more sustainably.

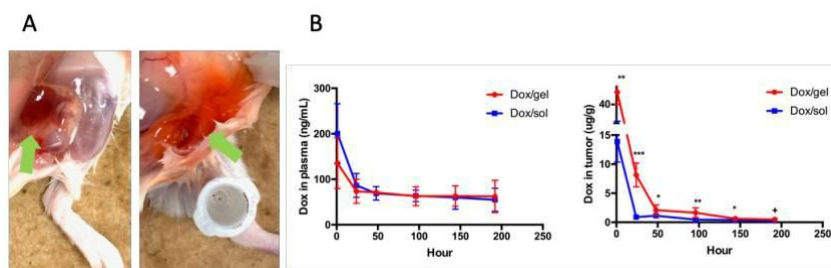


**Figure 4.** The Dox/gel reagent (left) maintained the hydrogel formation 1 hr post-injection and showed less diffusion into tissue compared to the dox/sol reagent (right) (A). Pharmacokinetics and biodistribution studies indicate less drug in plasma (left) and more in the tumor site (right) at initial time points when treating with the Dox-containing Ade-FFF hydrogel (B).

### 3. Conclusion

The controlled drug release from an Ade-FFF hydrogel was evaluated. By taking advantage of its nucleobase stacking structure in self-assembled nanofibers, we confirmed that the Ade-FFF hydrogel loads a high concentration of Dox (1 mM) and stores the drug without diffusive leakage. We measured an increased storage modulus when Dox was added to Ade-FFF hydrogels and its intercalation between adenine stacking structures was validated by a MD simulation. Dox release only occurred upon degradation of the Ade-FFF hydrogel and linear drug release was observed when the construct was degraded by proteinase K. In vitro studies in the presence of 4T1

cancer cells indicated Dox release at concentrations that initiate effective and sustained cancer cell death. *In vivo* experiments with tumor-bearing mice provided evidence of effective Dox release in tissue. Mice treated by injection of a Dox-containing Ade-FFF hydrogel carrier showed significantly decreased tumor size and weight compared to a Dox solution alone. Pharmacokinetics and biodistribution proved that drug retention is greater when incorporated in the nucleo-peptide hydrogel.

The use of nucleo-peptide hydrogels for drug delivery applications is a novel approach. We explored these self-assembled constructs and their physical, mechanical, and structural properties in our previous work and here extended those studies to report the first example of sustained release and antitumor efficacy of an injectable, chemotherapeutic-loaded nucleo-peptide-based hydrogel.<sup>17</sup> We further demonstrate more linear and sustained Dox release profile than has been reported previously with structurally similar short, self-assembling peptide systems.<sup>34</sup> Overall, the self-assembled Ade-FFF hydrogel showed significant potential for applications as a controlled drug release scaffold.

## **4. Experimental Sections**

### **4.1. Synthesis of nucleo-peptide**

The nucleo-peptide, Ade-FFF, was synthesized by a combination of solution and solid phase synthesis. First, Boc-protected adenine acetic acid was synthesized and then this molecule was used as a building block at the last coupling step of solid-phase peptide synthesis for N-terminal modification. Traditional fluorenylmethyloxycarbonyl (Fmoc) chemistry and diisopropylcarbodiimide (DIC)/ethyl 2-cyano-2-(hydroxyimino)acetate (OxymaPure) amide coupling chemistry were adopted for solid-phase peptide synthesis.

The primary amine of adenine was protected by tert-butyloxycarbonyl group. 1 equiv. of adenine, 0.1 equiv. of dimethylaminopyridine (DMAP), and 4 equiv. of Boc<sub>2</sub>O were dissolved in dry THF, and an overnight reaction at room temperature was performed. After evaporating excess THF in vacuo, the product was dissolved with saturated NaHCO<sub>3</sub> aq. in MeOH for and reacted at 50°C for 1 hr. Dichloromethane (DCM) extraction was applied (3 times) to separate the product from scavengers and the product was dried with Na<sub>2</sub>SO<sub>4</sub>, filtered, and evaporated.

Boc-protected adenine (1 equiv) was reacted with sodium hydride (1.2 equiv) and methyl bromoacetate (1 equiv) in THF initially at 0°C and then allowed to warm to room temperature overnight. The reaction was quenched by adding water and DCM extraction was performed (4 times) after evaporating excess THF. The dry product was collected and purified by normal-phase flash chromatography (silica gel column, ethyl acetate and hexane solvent system, 5% to 95% gradient).

The methyl protecting group of the acetate linker was deprotected in basic conditions (1.2 equiv of sodium hydroxide in H<sub>2</sub>O/THF solvent). After reacting for 30 minutes at 0 °C, 1N HCl was added dropwise to reduce the pH to 2-3. The reaction solution was then extracted by ethyl acetate (4 times). The final Boc-protected adenine acetic acid was obtained after drying and evaporating in vacuo.

To synthesize Ade-FFF (0.25mmol), Fmoc-Phe-Wang resin was used as a starting material for solid phase peptide synthesis. Resins were swelled in DCM and rinsed with DMF. Fmoc deprotection was performed by reacting with 20% piperidine in DMF for 20 minutes (2 times). After washing with DMF and DCM, a coupling solution (3 equiv of protected amino acid or nucleobase acetic acid, 3 equiv of OxymaPure, and 3 equiv of DIC) was added to the resin and reacted for 50 minutes. Resins were washed with DMF and DCM to remove excess coupling

reagents. This cyclic reaction was performed until the desired sequence was achieved: Ade-FFF attached to the resin. Protected nucleo-peptide was cleaved from the resin and deprotected by reacting with a 95:2.5:2.5 trifluoroacetic acid:water:triisopropylsilane cleavage cocktail for 2.5 hrs. The product-containing solution was collected, concentrated in vacuo, and precipitated as a white solid using cold diethyl ether. The solid product was washed with cold diethyl ether 3 times, dried over a stream of air, and then purified by reversed-phase HPLC. Briefly, a C18 column was flushed and cleaned at 95% acetonitrile (ACN). The dry crude product was then dissolved in a water:ACN (2:1) solution, injected into the pump, and loaded onto the column. A method was created manually to run an H<sub>2</sub>O:acetonitrile solvent at a gradient from 5% to 95% acetonitrile in water and a flow rate of 2 mL/min for one hour. Analyte peaks were detected at wavelengths of 214, 254, and 280 nm. Product-containing fractions were collected directly, filtered, and analyzed using an Agilent Technologies 6120 Single Quadrupole LC-MS autosampler. Samples were run on the same 5% to 95% acetonitrile in water gradient using an Agilent ZORBAX Eclipse Plus C18 narrow bore column at a 1.0 L injection volume and chromatogram peak areas were calculated to evaluate purity. Analytes were then ionized with an electrospray source. The instrument produces mass adducts in both positive and negative modes and a mass-adduct calculator facilitated product identification. Agilent ChemStation software provided chromatography peak outputs and mass spectra. Pure product (>95%) was lyophilized to achieve a solid powder of nucleo-peptide.

#### **4.2. Gelation of nucleo-peptide and loading reagents**

A pH switch method was adopted to trigger self-assembly of Ade-FFF. Ade-FFF powder was dissolved in basic aqueous solution (200 $\mu$ L H<sub>2</sub>O and 40 $\mu$ L 0.5M NaOH), and the solution was gently mixed until becoming clear. 0.5M of HCl was then added dropwise and the pH of the solution was monitored using pH paper. The pH was gradually reduced until the self-assembled structure was observed.

To load reagents into the Ade-FFF hydrogel, a concentrated solution of either Dox (for cancer drug) or DAPI (for dye) was prepared. After making the Ade-FFF hydrogel by pH switch (final pH was approximately 7.5), the reagent solution was added directly to the construct and gently mixed until becoming homogeneous. The solution mixture was then left on the lab bench at room temperature for about 5-10 minutes to recover its gelled structure.

#### **4.3. Mechanical properties analysis of Dox containing Ade-FFF hydrogel**

Mechanical properties of Ade-FFF hydrogels containing various concentrations of Dox were measured by an Anton-Paar MCR101 rheometer with a parallel plate geometry (8 mm top plate diameter). Shear stress rheometry was used to examine storage and loss modulus in the range of 0.5-100 Hz at 1% strain.

#### **4.4. Molecular dynamics (MD) simulation for Ade-FFF containing Dox**

Computational studies were performed to analyze the molecular interaction between Dox and Ade-FFF. AMBER 14 was used for the MD simulation with AMBERff12SB force field, periodic boundary conditions, and an explicit solvent system. Adenine acetic acid residue (ADL), C-terminal protonated phenylalanine (AHP), and doxorubicin (Dox)—all non-standard molecular structures in AMBER software—were parameterized before constructing the whole system. AM1-BCC and AMBER atom types were used for allocating charge and force field parameter to each

atom respectively.[25-27] AMBER GAFF force field was also adopted to solve missing parameters.[28] Individual Ade-FFF molecule were built by AMBER tleap with parameterized non-standard residues. (ADL-FF-AHP)

Packmol was used to construct an initial random structure possessing 60 molecules of Ade-FFF and 15 molecules of Dox in the simulation box (100 Å cube).[29] The system was solubilized by putting an appropriate number of TIP3P water molecules and ions, Na<sup>+</sup> and Cl<sup>-</sup>. Energy minimization and equilibrations were performed before the productive simulated annealing (SA) MD. 1000 cycles (500 by steepest descent and 500 by conjugate gradient algorithm) with solute restrain and 2500 cycles of full system minimization (1000 by steepest descent and 1500 by conjugate gradient algorithm) were initially performed to avoid high-energy contacts between molecules. A 100 ps NVT equilibration with solute restrain and 1 ns of the whole system NPT equilibration proceeded before the main SA MD simulation. 50 ns SA MD simulations to drive assembly was performed with a reduced temperature profile, starting from 300K, increasing to 500K during the initial 5 ns, then gradually decreasing to 300K during the next 40 ns, and maintaining 300K for the last 5 ns NPT equilibration. SHAKE algorithm was used to constrain covalent bonds containing hydrogen, allowing the time step to increase to 2 fs.[30] Langevin thermostat and Berendsen barostat were adopted to maintain constant temperature and pressure, respectively.[31,32]

#### **4.5. In vitro release analysis with various proteinase and cell environments**

Three conditions were used to evaluate the release profile of Dox from Ade-FFF hydrogels (1 mM Dox in 25 mM Ade-FFF hydrogel): PBS, trypsin (0.5%), and proteinase K (4 Unit/mL). 400 µL of Dox-containing hydrogels were made in a 1.2 mm diameter vial and then an equivalent volume of buffer with proper proteinase was added on top of the hydrogels. The vials were placed

in 37 °C incubator to maintain proteinase activity. 200 µL of supernatant was collected at specific timepoints and analyzed by UV spectrometer with absorbance set to 485 nm. Fresh buffered proteinase solution was added to the vial after sampling.

In vitro release to 4T1 mice cancer cells was also measured in order to investigate the effects on viability and to evaluate hydrogel degradation rate by multiple enzymes secreted by cells. Dox-containing hydrogels were formed in cell-culture inserts and equilibrated with complete media before starting the in vitro release experiment. 4T1 mice cancer cells, passaged at least twice before using, were seeded on the bottom of a 24 well plate at 5000 cells/mL. After incubating overnight, inserts containing drug-loaded hydrogels were placed in each well. MTS assays were performed at specific timepoints to analyze the proliferation of 4T1 cancer cells and the entrapped Dox inside the hydrogel was quantified by fluorescence spectrometer with excitation at 485 nm and emission at 590 nm.

#### **4.6. In vivo release analysis for tumor growth inhibition, histology, and immunohistochemical staining**

A mouse model (BALB/c) was chosen to evaluate *in vivo* continuous Dox release by Ade-FFF hydrogels, and all animal experiments used in this study were reviewed and approved based on ethical procedures and scientific care by the University of Texas at Austin Institutional Animal Care and Use Committee (IACUC). 4T1 metastatic mammary carcinoma (CRL-2539) cell lines were purchased from the American Type Culture Collection (ATCC).

The cytotoxicity of Ade-FFF hydrogel (25 mM) in the mouse model was determined before starting the Dox release experiment. 10 mice were randomly divided into two groups, PBS and Ade-FFF hydrogel. Each reagent—either 100 µL of PBS buffer or Ade-FFF hydrogel—was injected into the mice mammary fat pad. The health status of the mice, including weight, breath,

mobility, and food ingestion, was followed every day until day 7. The mice were sacrificed on day 7 and hematoxylin & eosin (H&E) histology was applied to evaluate the status of tissue in proximity to the reagents.

To investigate the effect of controlled release of Dox from the Ade-FFF hydrogel, 28 mice were randomly divided into four groups: controls (treated with PBS), Dox-only (treated with Dox solution), hydrogel-only (treated with hydrogel), and Dox/hydrogel (treated with Dox-loaded hydrogel). 4T1 cancer cells were injected into the mouse mammary fat pad ( $5 \times 10^5$  cells) in order to produce palpable tumors. After the tumor volume reached 100 mm<sup>3</sup>, 100  $\mu$ L of each respective agent (3 mg/kg of Dox was used in the case of Dox-containing reagent) was injected intratumorally. Tumor volumes of each group were measured every 2 days and mice were sacrificed on day 10 or day 12. Tumors were collected to determine weight and process immunohistochemical (IHC) staining.

Tumor tissue was embedded in optimal cutting temperature (OCT) compound and flash-frozen by using the isopropyl alcohol-dry ice bath. 10  $\mu$ m sections were cut using a Thermo Scientific CryoStar NX50 Cryostat, and immunohistochemical staining was performed to investigate caspase-3 mediated apoptosis in tumor tissues. Slides were fixed with formalin, washed with PBS two times, and then dried overnight at room temperature. Samples were rehydrated followed by antigen retrieval with sodium citrate buffer (pH 6.0) at 95 °C for 20 minutes. Staining reproduced the manufacturer's protocol of rabbit specific horseradish peroxidase (HRP)/diaminobenzidine (DAB) avidin-biotin complex (ABC) detection IHC kit (Abcam #ab64261). Slides were treated with a protein block solution containing 1/300 of cleaved caspase-3 (Asp 175) antibody (Cell Signaling Technology #9661) and incubated with the primary antibody

at 4 °C overnight.<sup>[33]</sup> The staining was developed by adopting DAB as a substrate and the slides were counterstained with hematoxylin. Bright-field microscopy was used for imaging analysis.

#### **4.7. Dox pharmacokinetics and biodistribution**

To evaluate the pharmacokinetics and biodistribution of Dox delivery by Ade-FFF hydrogels, 60 mice were randomly divided into two groups: controls (treated by aqueous Dox solution) and Dox/hydrogel (treated by Dox-containing Ade-FFF hydrogels). 4T1 cancer cells were injected into the mouse mammary fat pad ( $5 \times 10^5$  cells) to create tumors. After tumor volume reached 100 mm<sup>3</sup>, 100 μL of each respective agent was injected intratumorally. Mice from each group were sacrificed at specific timepoints—1 hour, day 1, day 2, day 4, day 6, and day 8—and their blood and organs (tumor, axillary and inguinal lymph nodes, liver, heart, and lung) were collected.

Dox in blood plasma and mice organs was quantified and analyzed according to the method in Mackay et al.<sup>[20]</sup> Initially, a Dox standard curve was profiled by measuring the fluorescence at a range of Dox concentrations (5 M to 3.125 nM). An acidified extraction solution (90% isopropanol and 10% 75 mM HCl) was used to extract Dox from plasma and organs. 100 μL of whole blood with heparin-containing solution (2 Units) was collected and plasma was separated by centrifugation at 14,000 rpm for 10 minutes. A volume of 50 μL plasma was mixed with 400 μL of acidified extraction solution and again centrifuged (14,000 rpm, 10 minutes). 200 μL of supernatant was collected and its fluorescence (excitation at 485 nm, emission at 590 nm) was measured. The weight of each organ was measured and subsequently homogenized with 1 mL of acidified extraction solution (2 mL was used for liver samples). 500 μL of homogenized solutions were centrifuged at 14,000 rpm for 10 minutes and then 200 μL of each supernatant was collected. Fluorescence was measured by the method above.

### Supporting Information

Supporting Information is available from the Wiley Online Library or from the author.

### Acknowledgements

This work was funded by the National Science Foundation (DMR-1609212).

Received:  
Revised:  
Published online:

### References

- [1] M. J. Webber, R. Langer, *Chem. Soc. Rev.* **2017**, *46*(21), 6600.
- [2] G. A. Hughes, in *Nanomedicine in Cancer*, Vol. 1 (Ed. L. P. Balogh), Pan Stanford, Singapore **2017**, pp. 47.
- [3] J. Li, D. J. Mooney, D. J., *Nature Rev. Mater.* **2016**, *1*(12), 16071.
- [4] M. W. Tibbitt, J. E. Dahlman, R. Langer, *J. Am. Chem. Soc.* **2017**, *138*(3), 704.
- [5] C. S. Brazel, N. A. Peppas, *J. Controlled Release* **1996**, *39*(1), 57.
- [6] M. Norouzi, B. Nazari, D. W. Miller, *Drug Discovery Today* **2016**, *21*(11), 1835.
- [7] S. Zhang, J. Ermann, M. D. Succi, A. Zhou, M. J. Hamilton, B. Cao, J. R. Korzenik, J. N. Glickman, P. K. Vemula, L. H. Glimcher, G. Traverso, *Sci. Transl. Med.* **2015**, *7*(300), 128.
- [8] Y. Jiang, J. Chen, C. Deng, E. J. Suuronen, Z. Zhong, *Biomaterials* **2014**, *35*(18), 4969.
- [9] Q. V. Nguyen, J. H. Park, D. S. Lee, *Eur. Polym. J.* **2015**, *72*, 602.
- [10] C. Yan, D. J. Pochan, *Chem. Soc. Rev.* **2010**, *39*(9), 3528.
- [11] J. Li, R. Xing, S. Bai, X. Yan, *Soft Matter* **2019**, *15*, 1704.
- [12] L. Haines-Butterick, K. Rajagopal, M. Branco, D. Salick, R. Rughani, M. Pilarz, J. P. Schneider, *Proc. Natl. Acad. Sci. U. S. A.* **2007**, *104*(19), 7791.
- [13] M. C. Branco, J. P. Schneider, *Acta Biomater.* **2009**, *5*(3), 817.

- [14] H. Acar, S. Srivastava, E. J. Chung, M. R. Schnorenberg, J. C. Barrett, J. L. LaBelle, M. Tirrell, *Adv. Drug. Delivery Rev.* **2017**, *110*, 65.
- [15] S. S. Liow, Q. Dou, D. Kai, Z. Li, S. Sugiarto, C. Y. Y. Yu, A. Kizhakeyil, *Small* **2017**, *13(7)*, 1603404.
- [16] T. Wu, B. Zhang, Y. Liang, T. Liu, J. Bu, L. Lin, X. Cai, *RSC Adv.* **2015**, *5(102)*, 84334.
- [17] K. Baek, A. D. Noblett, P. Ren, L. J. Suggs, *ACS Appl. Bio Mater.* **2019**, *2(7)*, 2812.
- [18] R. K. Ralph, B. Marshall, S. Darkin, *Trends Biochem. Sci.* **1983**, *8(6)*, 212.
- [19] K. M. Eckes, X. Mu, M. A. Ruehle, P. Ren, L. J. Suggs, *Langmuir* **2014**, *30(18)*, 5287.
- [20] J. A. MacKay, M. Chen, J. R. McDaniel, W. Liu, A. J. Simnick, A. Chilkoti, *Nat. Mater.* **2009**, *8(12)*, 993.
- [21] H. Saito, A. S. Hoffman, H. I. Ogawa, *J. Bioact. Compat. Polym.* **2007**, *22(6)*, 589.
- [22] M. Dadsetan, Z. Liu, M. Pumberger, C. V. Giraldo, T. Ruesink, L. Lu, M. J. Yaszemski,
- [23] L. Zhao, L. Zhu, F. Liu, C. Liu, Q. Wang, C. Zhang, J. Li, J. Liu, X. Qu, Z. Yang, *Int. J. Pharm.* **2011**, *410(1-2)*, 83.
- [24] S. Wang, E. A. Konorev, S. Kotamraju, J. Joseph, S. Kalivendi, B. Kalyanaraman, *J. Biol. Chem.* **2004**, *279(24)*, 25535.
- [25] D. A. Case, V. Babin, J. Berryman, R. M. Betz, Q. Cai, D. S. Cerutti, A. W. Goetz, *Amber 14* **2014**.
- [26] W. D. Cornell, P. Cieplak, C. I. Bayly, I. R. Gould, K. M. Merz, D. M. Ferguson, P. A. Kollman, *J. Am. Chem. Soc.* **1995**, *117(19)*, 5179.
- [27] A. Jakalian, D. B. Jack, C. I. Bayly, *J. Comput. Chem.* **2002**, *23(16)*, 1623.

- [28] J. Wang, R. M. Wolf, J. W. Caldwell, P. A. Kollman, D. A. Case, *J. Comput. Chem.* **2004**, *25(9)*, 1157.
- [29] L. Martínez, R. Andrade, E. G. Birgin, J. M. Martínez, *J. Comput. Chem.* **2009**, *30(13)*, 2157.
- [30] H. C. Andersen, *J. Comput. Phys.* **1983**, *52(1)*, 24.
- [31] S. E. Feller, Y. Zhang, R. W. Pastor, B. R. Brooks, *J. Chem. Phys.* **1995**, *103(11)*, 4613.
- [32] H. J. Berendsen, J. V. Postma, W. F. van Gunsteren, A. R. H. J. DiNola, J. R. Haak, *J. Chem. Phys.* **1984**, *81(8)*, 3684.
- [33] G. Cinar, A. Ozdemir, S. Hamsici, G. Gunay, A. Dana, A. B. Tekinay, M. O. Guler,
- [34] R. Ischakov, L. Adler-Abramovich, L. Buzhansky, T. Shekhter, E. Gazit, *Bioorg. Med. Chem.* **2013**, *21*, 3517.